Atmospheric Environment 233 (2020) 117532

Contents lists available at ScienceDirect

Atmospheric Environment

journal homepage: http://www.elsevier.com/locate/atmosenv

Black carbon and its impact on air quality in two semi-rural sites in Southern Italy near an oil pre-treatment plant

Giulia Pavese [a,*], Mariarosaria Calvello [a], Jessica Castagna [a], Francesco Esposito [b]

[a] Istituto di Metodologie per l'Analisi Ambientale-Consiglio Nazionale delle Ricerche, Ctr.da S. Loja, 85050, Tito Scalo (PZ), Italy
[b] Scuola di Ingegneria-Università della Basilicata, Ctr.da Macchia Romana, 85100, Potenza, Italy

HIGHLIGHTS

- Comparison of one-year EBC data from two semi-rural sites close to an oil pre-treatment plant (COVA) .
- Higher concentrations of pollutants from COVA emissions at the site closer to the plant.
- Additional domestic heating source at Grumento identified via AAE analysis.
- A procedure to identify the contribution of transboundary biomass burning.
- Double value of Passively liSmoked Cigarettes (2.8) obtained at COVA plant compared to Grumento (1.4) .

ARTICLE INFO

Keywords:
Equivalent black carbon
Oil plant
Air quality
Biomass burning
Passively smoked cigarettes

ABSTRACT

One-year-long data (October 2017–October 2018) of the equivalent black barbon (EBC), absorption Ångström exponent (AAE), and gaseous compound concentrations in two semi-rural sites in the Agri Valley, Southern Italy, were analyzed. This study aimed to assess the effects of combustion emissions on the air quality and people's health in these sites. The first measurement site, VZI, is located close to the plant, whereas the second is in Grumento, one of the towns at the edge of the valley, approximately 3 km away from the COVA. The emissions mainly originate from the biggest European on-shore pre-treatment plant of crude oil, the Centro Olio Val d'Agri (COVA), which hosts three incinerators and three torches continuously burning. EBC and gaseous pollutants from the COVA mainly affect the area close to the plant. A reduced effect is observed in Grumento where the AAE analysis highlighted the contribution of local domestic heating as an additional source during the cold season.

A procedure combining EBC measurements, high-resolution fire satellite visible/infrared imaging radiometer (VIIRS) data, and hybrid single-particle Lagrangian integrated trajectory (HYSPLIT) back-trajectories allowed the identification of the measurement days influenced by both regional and transboundary transport of biomass burning emissions. The identified days were mostly in July, August, and October 2018. The comparison between EBC and $PM_{2.5}$ data, only available for the Grumento site, showed a good correlation ($R^2 = 0.6$ on a yearly basis), revealing the relevant contribution of the EBC to the fine particulate matter at the site. Finally, a risk communication methodology was applied to associate the number of daily passively smoked cigarettes (PSC) to the measured EBC concentrations. The daily PSC were 2.8 for VZI, and 1.4 for Grumento, which are closer to the results at the remote sites (0.7) than those at the urban sites ($10.1 \leq PSC \leq 159.0$).

1. Introduction

Carbonaceous particles, generally called Black Carbon (BC), are a byproduct of incomplete combustion processes and are recognized to play a crucial role in climate change, owing to their absorption of solar radiation. Bond et al. (2013) calculated that they account for a total climate forcing of +1.1 Wm^{-2}. Ding et al. (2016) demonstrated that BC itself could influence the planetary boundary level (PBL) meteorology, enhancing haze pollution, and Talukdar et al. (2019) verified that, an increase in surface BC could affect the lower tropospheric instability. The typical dimension of BC particles ($d \leq 2.5$ μm) favors their transport from sources to remote areas. Xu et al. (2017) found that tropospheric BC in the Arctic was strongly affected by the anthropogenic emissions from eastern and southern Asia. Popovicheva et al. (2017) investigated

* Corresponding author. Ctr.da S. Loja, 85050, Tito Scalo (PZ), Italy.
E-mail address: giulia.pavese@imaa.cnr.it (G. Pavese).

https://doi.org/10.1016/j.atmosenv.2020.117532
Received 4 November 2019; Received in revised form 26 March 2020; Accepted 17 April 2020
Available online 4 May 2020

the role and identified the sources of BC at high northern latitudes by analyzing data from a ship measurement campaign. They found that gas flaring from the Yamal–Khanty–Mansiysk and Nenets–Komi regions has the largest contribution to the BC concentrations measured near the Kara strait. It is worth highlighting that BC deposition in the Arctic causes a reduction in the snow albedo and faster snow melting (Evans et al., 2017). During its lifetime cycle, BC can be covered by organics, bring sulphates and/or metal particles (Lettino et al., 2017; Bhandari et al., 2019) and seriously affect human health. In their review, Rohr and Wyzga (2012), suggest paying special attention to the carbonaceous component of particulate matter (PM), which is considered one of the major contributors to diseases.

Despite the established effects of BC on climate, air quality and health, no regulatory limits of the BC concentration exist in Europe. Furthermore, few long-term data-sets of BC concentrations in Europe and the Mediterranean region have been published; some can be found in Querol et al. (2013), Sandrini et al. (2014), Calvello et al. (2015), and Kutzner et al. (2018).

In this study, we analyzed, compared, and discussed one-year EBC measurements collected simultaneously in two sites in the Agri Valley, a semi-rural area in Southern Italy. This area hosts few villages and the biggest European on-shore pre-treatment plant of crude oil in a populated area. One measurement site is close to the plant, and the other is in one of the villages located on the edge of the valley. In addition to local sources, the possible transport of carbonaceous particles originated by biomass burning and/or flaring phenomena was considered by applying a suitable procedure to both data-sets. The analysis allowed the evaluation of the effect of EBC's local sources on both sites. The sources were the oil plant and vehicular traffic in one site, and the oil plant and domestic heating in the other site. Finally, to assess the potential health risk associated with the EBC concentrations measured at the two sites, the EBC concentrations were converted into PSC values, via the method developed by Van der Zee et al. (2016).

2. Measurements, sites, and methods

The Agri Valley covers an area of approximately 1400 km^2, in the Basilicata region (Southern Italy). It is surrounded by the Agri Valley and Lagonegrese National Park. Few towns are located in the valley, hosting approximately 50,000 inhabitants. Agriculture had been the main activity until 1996, when drilling activities began and the biggest European on-shore pre-treatment plant of crude oil (180.000 m^2), the COVA plant, managed by ente nazionale idrocarburi (ENI) Italian company, was built. Currently, 24 oil wells producing 104.000 oil barrels per day are active in this area. The plant continuously emits BC from three security torches and three incinerators. An additional source of BC, as described in Calvello et al. (2014), is the SS598 national road (2900 vehicles per day, https://www.stradeanas.it/sites/default/files/Anas%20Dati%20TGMA%202017.pdf) running 1 km away from the COVA. During winter, another BC source could be domestic heating from the urbanized sites.

The peculiar characteristics of this area, where the oil plant is nearby some villages, suggested to focus on the analysis of continuous EBC concentrations measurements in VZI (40.31° N, 15.89° E, 594 m a.s.l.), a site very close to the COVA, and Grumento (40.29° N, 15.89° E, 746 m a.s.l.), a village on one edge of the valley. Measurements of gaseous

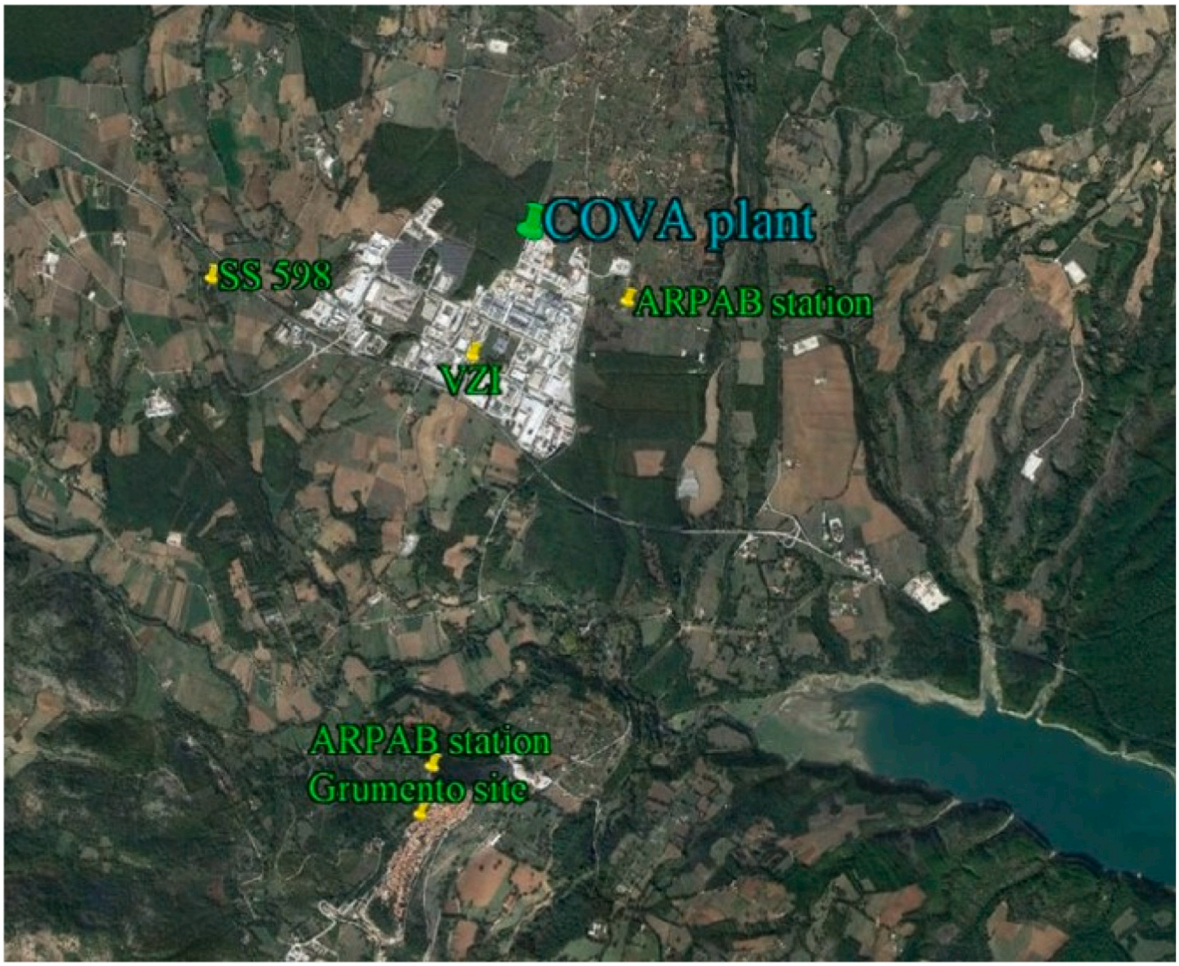

Fig. 1. Locations of the measurement sites in the Agri Valley.

pollutants and meteorological parameters from the Regional Agency for the Environment of Basilicata (ARPAB) were also considered to support the EBC measurement analysis in both sites. In Fig. 1, the area hosting the COVA plant together with the measurement sites and the ARPAB stations are shown. The EBC measurement sites are approximately 2800 m away from each other in a straight line, whereas the reference ARPAB stations are far approximately 900 and 350 m away from VZI and from Grumento, respectively. The data were collected from October 2017 to October 2018.

The ARPAB stations provide hourly mean concentrations of gaseous pollutants, such as sulfur dioxide (SO_2), carbon monoxide (CO), nitrogen dioxide (NO_2), hydrogen sulfide (H_2S), methane (CH_4), non-methane hydrocarbons (NMHCs) and benzene (C_6H_6) which were considered in this study. The ARPAB stations also provide the main meteorological parameters (temperature, relative humidity, wind velocity and direction). In addition, the Grumento ARPAB site only provides measurements of $PM_{2.5}$ and PM_{10}. Details on the ARPAB instruments can be found in Calvello et al. (2014).

EBC data were obtained with two MAGEE aethalometers (AE33 model) equipped with seven lamps (λ = 370, 470, 520, 590, 660, 880, 950 nm), whose emitted radiation is attenuated by BC particles deposited on a quartz fiber filter. According to the MAGEE manufacturer, the mass absorption cross-section (MAC) is 7.77 m^2g^{-1} at 880 nm and is inversely dependent on the wavelength. Atmospheric particulate matter was sampled using a $PM_{2.5}$ head, with a measurement time resolution of 1 min, although the analysis of both EBC data-sets was performed on an hourly basis. It is worth noting that the new seven-wavelength aethalometer (AE33 model) avoids the shadowing effect owing to the dual-spot technology (Drinovec et al., 2015) employed. The VZI and Grumento data-sets contain measurements from 348 to 384 days, respectively. A best-fit technique was applied to the absorption coefficients $\sigma_a(\lambda)$, to provide the estimate of the AAE and its variations to obtain information on different combustion processes (Esposito et al., 2012; Ran et al., 2016).

The EBC data-sets were also considered for the application of a suitable procedure (Castagna et al., 2019) that combines EBC measurements, high resolution VIIRS satellite data (Schroeder and Giglio, 2015) and HYSPLIT back trajectories (Stein et al., 2015) to investigate the possible influence of the transport of biomass burning and flaring pollutants on the EBC content at the measurement sites.

The EBC concentrations measured at both sites were also considered to assess the potential health risk, following the communication risk methodology developed by Van der Zee et al. (2016). This methodology associates the estimated risk from EBC exposure to that from PSC for four outcome measures, namely: low birth weight, decrease lung function (FEV1), cardiovascular mortality and lung cancer, averaged with suitable weight factors to obtain a single factor used to convert EBC concentrations into PSC.

3. Results and discussions

3.1. EBC data-sets analysis at VZI and Grumento sites

Fig. 2a and b shows the daily mean values of EBC and AAE at the VZI and Grumento sites. At first glance the EBC values in VZI are systematically higher than in Grumento, suggesting a stronger impact of the COVA emissions in the area close to the plant, as it would be expected.

Similar patterns of EBC concentrations underlined by black ellipses with different relative intensities, can be recognized at both sites, highlighting the different impacts of the COVA plant emissions in that area, owing to the pollutant diffusion effect. A substantial difference in the AAE parameter behavior is observed depending on the site: an evident seasonal pattern with higher values during winter is observed in Grumento but not VZI.

The most common statistical parameters (mean and standard deviations) were calculated for both EBC and AAE on a yearly time scale and for cold (October–March) and warm (April–September) seasons, as reported in Table 1. In VZI significantly higher EBC values were recorded for the warm season, as previously assessed for the years 2011–2013 (Calvello et al., 2015), whereas no significant seasonal difference was found in Grumento. In contrast, the AAE does not show substantial differences in VZI, with a yearly average value of 1.27 ± 0.12, which is close to the value of 1.2 reported by Lack and Langridge (2013) for BC coated with significant amounts of organic matter. The slightly higher value of 1.34 ± 0.12 in the cold season, partly due to the meteorological conditions favoring BC coating, is comparable to the value of 1.4 obtained by in-situ aircraft EBC measurements of flare plumes in the Bakken formation in North Dakota (Weyant et al., 2016). On the other hand, a considerable difference between warm (1.33 ± 0.20) and cold (1.99 ± 0.17) seasons is observed in Grumento. These values suggest

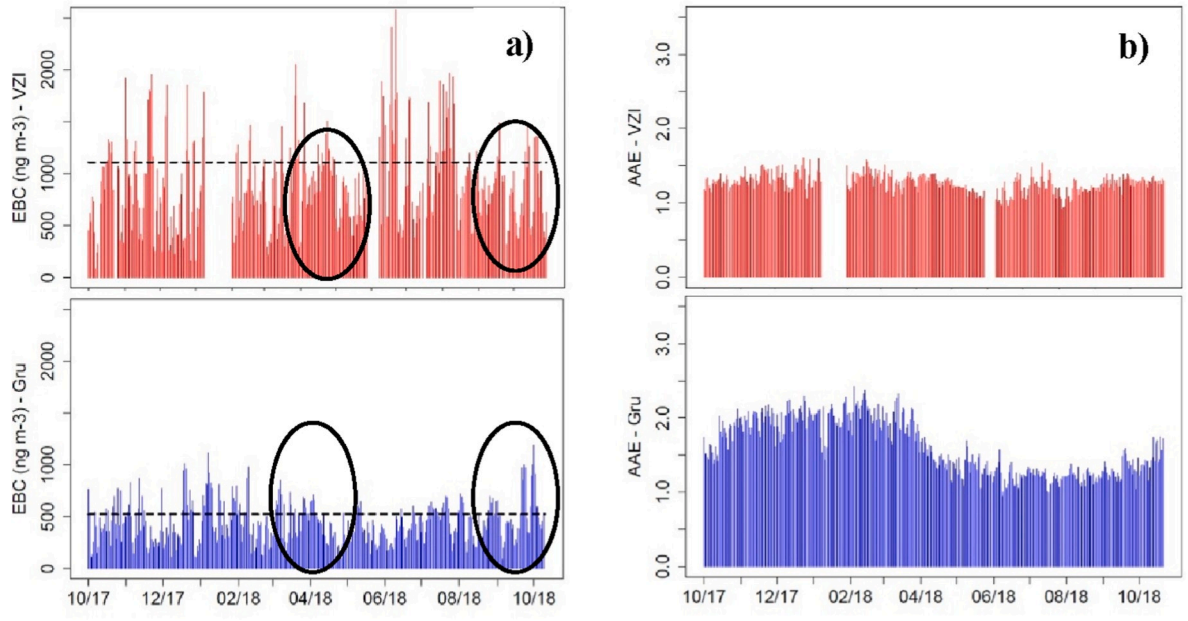

Fig. 2. Daily mean EBC (a) and AAE (b) values in VZI and Grumento. In (a), the dotted black line represents the 75° percentile calculated over the entire data-set.

Table 1
Main statistical parameters for EBC (a) and AAE (b) in VZI and Grumento for the whole data-set and for cold and warm seasons.

a) EBC		Mean (ng/m^3)	SD (ng/m^3)	Min. (ng/m^3)	Max. (ng/m^3)
VZI	**Year**	867	411	160	2408
	Cold	806	427	160	2055
	Warm	931	399	320	2408
Grumento	**Year**	421	186	88	1188
	Cold	404	179	110	1188
	Warm	403	152	88	735
b) AAE		Mean	SD	Min.	Max.
VZI	**Year**	1.27	0.12	0.92	1.60
	Cold	1.34	0.12	1.06	1.60
	Warm	1.22	0.11	0.92	1.53
Grumento	**Year**	1.61	0.37	0.95	2.42
	Cold	1.99	0.17	1.44	2.42
	Warm	1.33	0.20	0.95	2.14

that, during the cold season, the local residential biomass combustion is the dominating BC source in Grumento. Similar AAE values were in fact attributed to wintertime biomass burning at several sites worldwide ($1.68 < AAE < 1.82$) by Dumka et al. (2019), Martinsson et al. (2017), Mousavi et al. (2019), Zhang et al. (2017), and Zotter et al. (2017).

A correlation between the two data-sets was observed, considering both hourly mean and daily mean EBC values, as illustrated in Fig. 3 a-d.

These plots indicate different correlations depending on the time scale. For hourly mean data a poor correlation is found ($R^2 = 0.19$) due to the time-shift in the EBC patterns in Grumento compared with the COVA area. For daily mean data, a better correlation is observed as a result of a probable BC dilution over the valley over the day ($R^2 = 0.46$). An improved correlation is obtained considering the cold (October–March) and the warm (April–September) seasons. The corresponding scatter-plots are reported in Fig. 3c and d where the correlation coefficients are $R^2 = 0.61$ and $R^2 = 0.46$, respectively.

An ad-hoc procedure (Castagna et al., 2019) was applied to the EBC data-sets to verify the influence of transported biomass burning and/or flaring emissions. To this end, a subset of measurement days fulfilling the condition of EBC peaks higher than the 75th percentile (VZI 1122 ng/m^3, 87 days out of 348; Grumento 528 ng/m^3, 83 days out of 384) were considered. For these days, the VIIRS thermal anomalies were overlapped with the calculated HYSPLIT back-trajectories (ending point 500 m) arriving in VZI and Grumento under the following constraints: the back-trajectory must have moved into the boundary layer when overpassing the fire, and its distance from the fire must have been ≤ 750 m (1°). The result is a list of hotspots (fires and flaring emissions) potentially contributing to the measured EBC intense load, together with the map of the back-trajectories and intercepted fires. HYSPLIT back-tajectories calculated for both the measurement sites gave very similar results: July, August, and October 2018 were identified as the months most affected by biomass burning emissions occurring at both local (Southern Italy) and non-local scale (Eastern Europe). In a limited number of cases, the flaring emissions from the COVA, North African (Algeria and Libya), and Sicilian refineries were detected. Some examples of the output maps of the procedure for the VZI site are reported in Fig. 4 a-c. It is worth to note that the same results were obtained for the Grumento site.

3.2. EBC and air quality

Based on the gaseous pollutant concentrations and wind speeds and directions measured by ARPAB, an overview of the gaseous emissions in VZI and Grumento is presented in Fig. 5 a-f, where bivariate polar plots centered over the ARPAB stations receptor sites, for C_6H_6, H_2S, SO_2, CH_4, NMHC, and NO_2 are shown. For VZI, almost all pollutants show the highest concentrations for wind blowing from the COVA direction (W, N–W). In the case of NO_2, increased concentrations correspond to wind blowing from W/S–W, implying the additional contribution of traffic from the main road SS598.

Considering that the plots in Fig. 5 a-f have the same scale for both sites, higher concentrations of gaseous pollutants are evident in VZI, confirming a stronger influence of the COVA emissions on air quality in the proximity of the plant. In Grumento, a more homogeneous

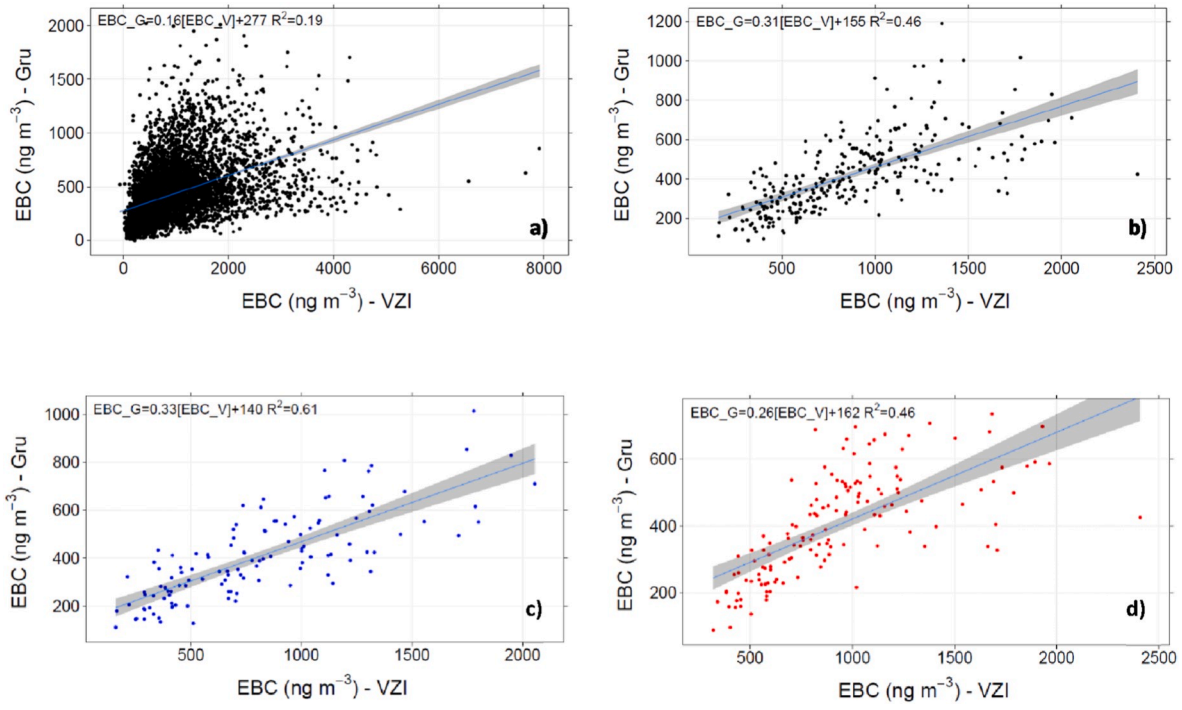

Fig. 3. a) Hourly (VZI vs. Grumento sites) EBC scatter-plot for the whole data-set. b) Daily EBC scatter-plot for the whole data-set. c) Daily EBC scatter-plot for the cold season. d) Daily EBC scatter-plot for the warm season.

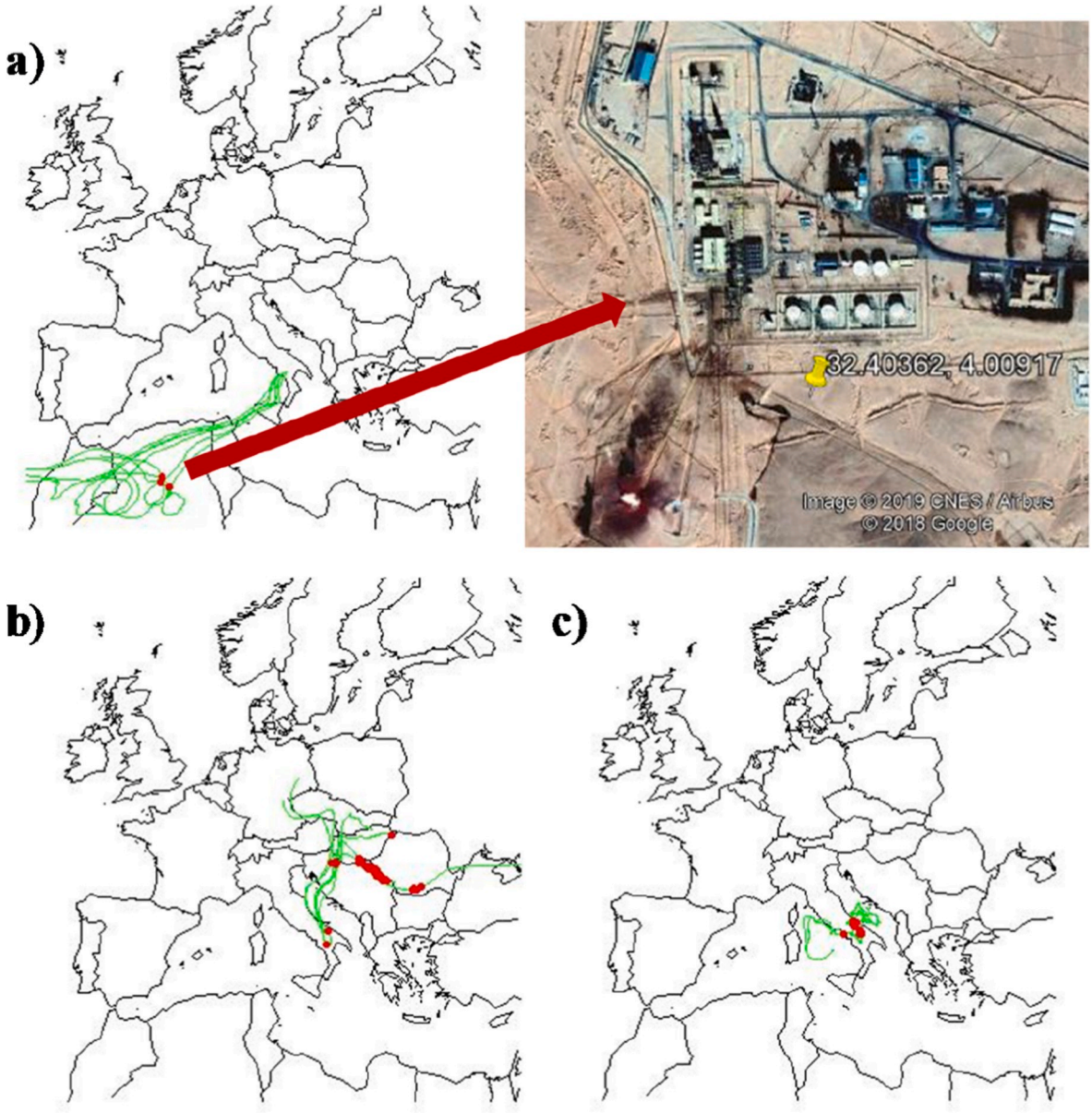

Fig. 4. Examples of output maps of the procedure. Detection of a) flaring from Algerian refineries on March 16, 2018 (the image on the right was obtained from Google Earth), b) regional and transboundary biomass burning on October 21, 2018, c) regional fires on August 11, 2018.

distribution of pollutants is observed, except for SO_2 and CH_4 which show slightly higher values in correspondence of Northerly winds coming from the COVA.

The correlation between EBC and $PM_{2.5}$ data were calculated only for the Grumento site, where $PM_{2.5}$ and PM_{10} measurements were available. The average yearly $PM_{2.5}$ to PM_{10} ratio is 58% which remains constant also when considering the cold and warm seasons. This result suggests prevailing fine particles regardless of the period of the year due to the combined influence of sources from the COVA area, local sources (domestic heating during the cold season and increased local vehicular traffic during summer), and transported biomass burning/flaring products. These results are confirmed by the high correlation observed between daily EBC and $PM_{2.5}$ data, as presented in yearly ($R^2 = 0.6$) and seasonal ($R^2 = 0.63$ cold season, $R^2 = 0.55$ warm season) scatter-plots of Fig. 6 a-c.

In most cases of high $PM_{2.5}/PM_{10}$ ratio ($\geq$70%), the EBC peaks exceeded the 75th percentile (528 ng/m^3), confirming that the $PM_{2.5}$ increase was directly related to the increase in BC which, therefore, can be considered one of the main components of fine particulate matter. Among all cases, three were considered to describe this effect on the air quality in Grumento: on January 14, 2018 ($PM_{2.5}/PM_{10}$ = 83%, EBC = 655 ng/m^3) with domestic heating probably dominating BC emissions; on August 23, 2018 ($PM_{2.5}/PM_{10}$ = 94%, EBC = 691 ng/m^3) when a local festival caused an augmented vehicular traffic; and on October 14, 2018 ($PM_{2.5}/PM_{10}$ = 79%, EBC = 972 ng/m^3) when transported biomass burning byproducts reached the site, as verified by the above-mentioned procedure. Fig. 7 shows the output of the procedure for October 14, 2018, revealing the presence of numerous fires along the air mass pathway over Eastern Europe.

3.3. EBC and health risk communication methodology

Owing to the lack of a legislative limit of the BC value, the effective communication of the possible impacts of BC on health is still a challenging task. Van der Zee et al. (2016) addressed this issue by proposing a risk communication methodology whereby the effects of some air

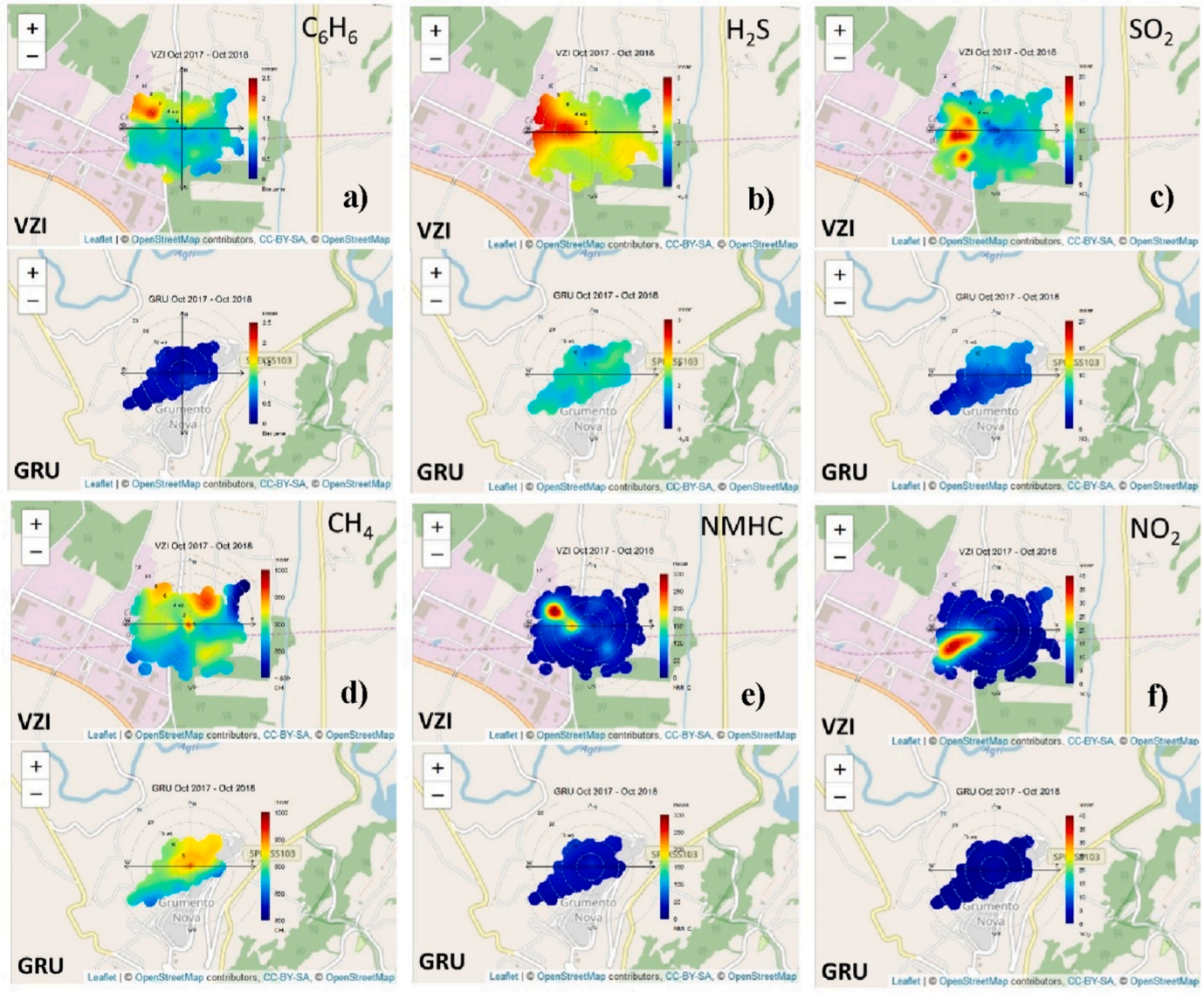

Fig. 5. Polar plots at the receptor sites (VZI and Grumento) of gaseous pollutants (a) C_6H_6, (b) H_2S, (c) SO_2, (d) CH_4, (e) NMHC and (f) NO_2, typical of both COVA and vehicular traffic emissions.

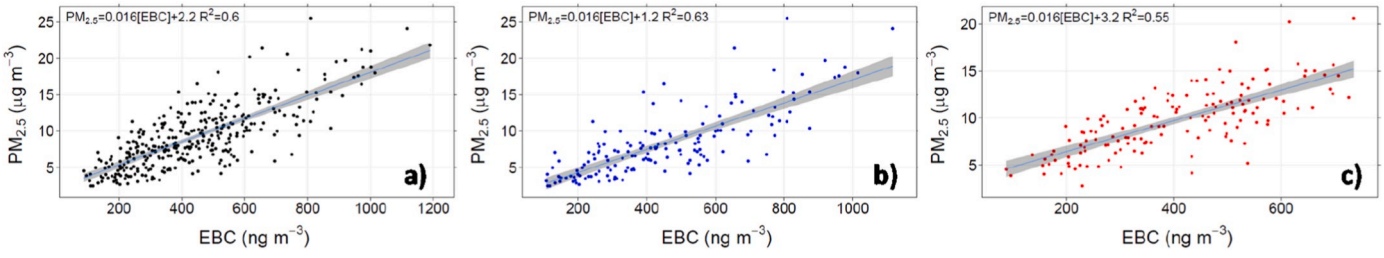

Fig. 6. Scatter plots of $PM_{2.5}$ vs. EBC measured over the year (a) and for cold (b) and warm (c) seasons at Grumento.

pollutants (NO_2, $PM_{2.5}$ and BC) on health are converted in the number of daily PSC that have those effects. The authors considered the health outcomes strictly related to both tobacco smoke exposure and air pollution: low birth weight, decreased lung function, cardiovascular mortality and lung cancer. Following the calculation of Van der Zee et al. (2016), the EBC concentrations in VZI and Grumento were expressed into daily PSC assuming an average number of 11.3 smoked cigarettes per day in the Basilicata Region (Istat, 2016, https://www.istat.it/it/archivio/202040), instead of the value of 14 used by Van der Zee et al. (2016). The results are listed in Table 2 together with the number of daily PSC calculated in other sites in the world (Van der Zee et al., 2016 and Wu et al., 2018). The PSC value calculated in VZI is twice that calculated in Grumento, indicating a stronger effect of anthropogenic activities on air quality close to the emission site. These values are much more similar to that obtained at the remote site of Ny Ålesund than those obtained in other urban sites worldwide.

Fig. 7. Output of the procedure detecting the influence of biomass burning on EBC concentrations measured on October 14, 2018. The 500 m a.g.l. back trajectory, moving within the boundary layer, intercepts many fires.

Table 2
Estimated PSC corresponding to the EBC values measured in this and previous works.

Site	Reference	# Passively Smoked Cigarettes
VZI - Italy	This work	2.8 ± 2.2
Grumento - Italy	This work	1.4 ± 1.1
Amsterdam-Netherlands	Van der Zee et al. (2016)	10.1 ± 1.8
Karachi - Pakistan	Wu et al. (2018)	159.0 ± 119.5
Tijuana - Mexico	Wu et al. (2018)	83.0 ± 62.3
Dakar - Senegal	Wu et al. (2018)	60.5 ± 45.5
Granada - Spain	Wu et al. (2018)	33.3 ± 25.1
Milan - Italy	Wu et al. (2018)	24.1 ± 18.1
Xining - China	Wu et al. (2018)	11.1 ± 8.3
Ny Ålesund - Norway	Wu et al. (2018)	0.7 ± 0.5

4. Conclusions

BC and its effects on both air quality and health in two semi-rural sites in the Agri Valley (Southern-Italy) were studied over a one-year period. The first site, VZI, is close to the biggest European on-shore pre-treatment plant of crude oil, whereas the second, Grumento, is one of the villages of the valley. The main achievements of this study can be summarized as follows:

- Daily EBC measurements showed similar patterns in both sites, with systematic lower intensities in Grumento, highlighting the contribution of the COVA area emissions on BC. Good correlations between EBC concentrations measured in VZI and Grumento were found both for the whole year ($R^2 = 0.46$), and for the warm ($R^2 = 0.46$) and cold ($R^2 = 0.61$) seasons.
- The AAE values obtained during winter in Grumento, allowed the identification of the contribution of local domestic heating to the EBC concentrations. The AAE exhibited a seasonal trend only in Grumento, with higher values during the cold season.
- The application of a procedure combining ground-based and satellite data, allowed the identification of the measurement days affected by biomass burning emissions at both regional and transboundary scales, mainly during July, August, and October 2018.
- The analysis of the bivariate polar plots of gaseous pollutants (C_6H_6, H_2S, SO_2, CH_4, NMHC) revealed a stronger impact in the area close to the COVA source. In contrast, NO_2 emissions were mainly originated from the vehicular traffic.
- Measurements of $PM_{2.5}$ and PM_{10} which were available only in Grumento, indicated a high $PM_{2.5}$ to PM_{10} ratio (58% on a yearly basis). Moreover, a high correlation between $PM_{2.5}$ and EBC ($R^2 = 0.6$ yearly) was found, suggesting BC as one of the main components of fine particulate matter.
- The risk communication methodology proposed by Van der Zee et al. (2016) was used to express the health effect of BC in terms of the number of daily PSC. The value obtained in VZI (PSC = 2.8) was twice as large as that obtained in Grumento (PSC = 1.4). However, in both cases, these values were more similar to that obtained in a remote site (0.7) than those obtained in urban sites worldwide ($10.1 = PSC \leq 159$).

In summary, the EBC experimental data, a procedure allowing the identification of biomass burning products transport, and an estimation of the risk of EBC emissions to human health in terms of PSC lead to a comprehensive description of the impacts of EBC on air quality in the Agri Valley.

Declaration of competing interest

The authors declare that they have no known competing financial interests or personal relationships that could have appeared to influence the work reported in this paper.

CRediT authorship contribution statement

Giulia Pavese: Conceptualization, Writing - original draft, Funding acquisition, Supervision. **Mariarosaria Calvello:** Conceptualization, Formal analysis, Writing - original draft. **Jessica Castagna:** Formal analysis. **Francesco Esposito:** Data curation.

Acknowledgement

The authors acknowledge the use of data and imagery from Lance FIRMS operated by NASA's Earth Science Data and Information System (ESDIS) with funding provided by NASA Headquarter.

The authors gratefully acknowledge the NOAA Air Resources Laboratory (ARL) for the provision of the HYSPLIT transport and dispersion model and/or READY website (http://www.ready.noaa.gov) used in this publication.

Appendix A. Supplementary data

Supplementary data to this article can be found online at https://doi.org/10.1016/j.atmosenv.2020.117532.

Funding

This work was partly supported by the Smart Basilicata project (PON 04A200165), funded by the Italian Ministry of Education, University, and Research and the 2007–2013 Basilicata Regional Authority Cohesion Fund, and partly supported by the INDICARE cooperation agreement funded by the Fondazione Osservatorio Ambientale Regionale della Basilicata.

References

Bhandari, J., China, S., Chandrakar, K.K., Kinney, G., Cantrell, W., Shaw, R.A., Mazzoleni, L.R., Girotto, G., Sharma, N., Gorkowski, K., Gilardoni, S., Decesari, S., Facchini, M.C., Zanca, N., Pavese, G., Esposito, F., Dubey, M.K., Aiken, A.C., Chakrabarty, R.K., Moosmüller, H., Onasch, T.B., Zaveri, R.A., Scarnato, B.V., Fialho, P., Mazzoleni, C., 2019. Extensive soot compaction by cloud processing from laboratory and field observations. Sci. Rep. 9 (2019), 11824. https://doi.org/10.1038/s41598-019-48143-y.

Bond, T.C., Doherty, S.J., Fahey, D.W., Forster, P.M., Berntsen, T., De Angelo, B.J., Flanner, M.G., Ghan, S., Kärcher, B., Koch, D., Kinne, S., Kondo, Y., Quinn, P.K., Sarofim, M.C., Schultz, M.G., Schulz, M., Venkataraman, C., Zhang, H., Zhang, S., Bellouin, N., Guttikunda, S.K., Hopke, P.K., Jacobson, M.Z., Kaiser, J.W., Klimont, Z., Lohmann, U., Schwarz, J.P., Shindell, D., Storelvmo, T., Warren, S.G., Zender, C.S., 2013. Bounding the role of black carbon in the climate system: a scientific assessment. J. Geophys. Res. Atmos. 118, 5380–5552. https://doi.org/10.1002/jgrd.50171.

Calvello, M., Esposito, F., Trippetta, S., 2014. An integrated approach for the evaluation of technological hazard impacts on air quality: the case of the Val d'Agri oil/gas plant. Nat. Hazards Earth Syst. Sci. 14, 2133–2144. https://doi.org/10.5194/nhess-14-2133-2014.

Calvello, M., Esposito, F., Lorusso, M., Pavese, G., 2015. A two-year database of BC measurements at the biggest European crude oil pre-treatment plant: a comparison with organic gaseous compounds and PM10 loading. Atmos. Res. 164–165, 156–166. https://doi.org/10.1016/j.atmosres.2015.05.004.

Castagna, J., Calvello, M., Esposito, F., Pavese, G., 2019. Analysis of equivalent black carbon multi-year data at an oil pre-treatment plant: integration with satellite data to identify black carbon transboundary sources. Remote Sens. Environ. 235 (2019), 111429. https://doi.org/10.1016/j.rse.2019.111429.

Ding, A.J., Huang, X., Nie, W., Sun, J.N., Kerminen, V.-M., Petäjä, T., Su, H., Cheng, Y.F., Yang, X.-Q., Wang, M.H., Chi, X.G., Wang, J.P., Virkkula, A., Guo, W.D., Yuan, J., Wang, S.Y., Zhang, R.J., Wu, Y.F., Song, Y., Zhu, T., Zilitinkevich, S., Kulmala, M., Fu, C.B., 2016. Enhanced haze pollution by black carbon in megacities in China. Geophys. Res. Lett. 43, 2873–2879. https://doi.org/10.1002/2016GL067745.

Drinovec, L., Močnik, G., Zotter, P., Prévôt, A.S.H., Ruckstuhl, C., Coz, E., Rupakheti, M., Sciare, J., Müller, T., Wiedensohler, A., Hansen, A.D.A., 2015. The "dual-spot" Aethalometer: an improved measurement of aerosol black carbon with real-time loading compensation. Atmos. Meas. Tech. 8, 1965–1979. https://doi.org/10.5194/amt-8-1965-2015.

Dumka, U.C., Tiwari, S., Kaskaoutis, D.G., Devara, P.C.S., Kumar, R., Kumar, S., Tiwari, S., Gerasopoulos, E., Mihalopoulos, N., 2019. Year-long variability of the fossil fuel and wood burning black carbon components at a rural site in southern Delhi outskirts. Environ. Sci. Pollut. Res. 26, 3771. https://doi.org/10.1007/s11356-018-3885-y.

Esposito, F., Calvello, M., Gueguen, E., Pavese, G., 2012. A new algorithm for brown and black carbon identification and organic carbon detection in fine atmospheric aerosols by a multi-wavelength aethalometer. Atmos. Meas. Tech. Discuss. 5, 1003–1027. https://doi.org/10.5194/amtd-5-1003-2012.

Evans, M., Kholod, N., Kuklinski, T., Denysenko, A., Smith, S.J., Staniszewski, A., Hao, W.M., Liu, L., Bond, T.C., 2017. Black carbon emissions in Russia: a critical review. Atmos. Environ. 163, 9–21. https://doi.org/10.1016/j.atmosenv.2017.05.026.

Istat, 2016. last access. https://www.istat.it/it/archivio/202040. (Accessed 16 September 2019).

Kutzner, R.D., von Schneidemesser, E., Kuika, F., Quedenau, J., Weatherhead, E.C., Schmale, J., 2018. Long-term monitoring of black carbon across Germany. Atmos. Environ. 185, 41–52. https://doi.org/10.1016/j.atmosenv.2018.04.039.

Lack, D.A., Langridge, J.M., 2013. On the attribution of black and brown carbon light absorption using the Ångström exponent. Atmos. Chem. Phys. 13, 10535–10543. https://doi.org/10.5194/acp-13-10535-2013.

Lettino, A., Calvello, M., Esposito, F., Fiore, S., Lorusso, M., Pavese, G., 2017. Effects of polluted air-masses advection on atmospheric particles in a semi-rural site in South Italy by SEM-EDX analysis. Aerosol Air Qual. Res. 17, 69–83. https://doi.org/10.4209/aaqr.2016.05.0216.

Martinsson, J., Abdul Azeem, H., Sporre, M.K., Bergström, R., Ahlberg, E., Öström, E., Kristensson, A., Swietlicki, E., Eriksson Stenström, K., 2017. Carbonaceous aerosol source apportionment using the Aethalometer model–evaluation by radiocarbon and levoglucosan analysis at a rural background site in southern Sweden. Atmos. Chem. Phys. 17, 4265–4281. https://doi.org/10.5194/acp-17-4265-2017.

Mousavi, A., Sowlat, M.H., Lovett, C., Rauber, M., Szidat, S., Boffi, R., Borgini, A., De Marco, C., Ruprecht, A.A., Sioutas, C., 2019. Source apportionment of black carbon (BC) from fossil fuel and biomass burning in metropolitan Milan, Italy. Atmos. Environ. 203 (2019), 252–261. https://doi.org/10.1016/j.atmosenv.2019.02.009.

Popovicheva, O.B., Evangeliou, N., Eleftheriadis, K., Kalogridis, A.C., Sitnikov, N., Eckhardt, S., Stohl, A., 2017. Black carbon sources constrained by observations in the Russian high arctic. Environ. Sci. Technol. 51, 3871–3879. https://doi.org/10.1021/acs.est.6b05832.

Querol, X., Alastuey, A., Viana, M., Moreno, T., Reche, C., Minguillon, M.C., Ripoll, A., Pandolfi, M., Amato, F., Karanasiou, A., Perez, N., Pey, J., Cusack, M., Vazquez, R., Plana, F., Dall'Osto, de la Rosa, M.J., Sanchez de la Campa, A., Fernandez-Camacho, R., Rodrıguez, S., Pio, C., Alados-Arboledas, L., Titos, G., Artıñano, B., Salvador, P., Garcıa Dos Santos, S., Fernandez Patier, R., 2013. Variability of carbonaceous aerosols in remote, rural, urban and industrial environments in Spain: implications for air quality policy. Atmos. Chem. Phys. 13, 6185–6206. https://doi.org/10.5194/acp-13-6185-2013.

Ran, L., Deng, Z.Z., Wang, P.C., Xia, X.A., 2016. Black carbon and wavelength-dependent aerosol absorption in the North China Plain based on two-year aethalometer measurements. Atmos. Environ. 142, 132–144. https://doi.org/10.1016/j.atmosenv.2016.07.014.

Rohr, A.C., Wyzga, R.E., 2012. Attributing health effects to individual particulate matter constituents. Atmos. Environ. 62, 130–152. https://doi.org/10.1016/j.atmosenv.2012.07.036.

Sandrini, S., Fuzzi, S., Piazzalunga, A., Prati, P., Bonasoni, P., Cavalli, F., Bove, M.C., Calvello, M., Cappelletti, D., Colombi, C., Contini, D., de Gennaro, G., Di Gilio, A., Fermo, P., Ferrero, L., Gianelle, V., Giugliano, M., Ielpo, P., Lonati, G., Marinoni, A., Massabò, D., Molteni, U., Moroni, B., Pavese, G., Perrino, C., Perrone, M.G., Perrone, M.R., Putaud, J.-P., Sargolini, T., Vecchi, R., Gilardoni, S., 2014. Spatial and seasonal variability of carbonaceous aerosol across Italy. Atmos. Environ. 99, 587–598. https://doi.org/10.1016/j.atmosenv.2014.10.032.

Schroeder, W., Giglio, L., 2015. NASA VIIRS Land Science Investigator Processing System (SIPS) Visible Infrared Imaging Radiometer Suite (VIIRS) 375 M & 750 M Active Fire Products, Product User's Guide Version 1.4 available at: https://viirsland.gsfc.nasa.gov/PDF/VIIRS_activefire_User_Guide.pdf. (Accessed 16 September 2019).

Stein, A.F., Draxler, R.R., Rolph, G.D., Stunder, B.J.B., Cohen, M.D., Ngan, F., 2015. NOAA's HYSPLIT atmospheric transport and dispersion modeling system. Bull. Am. Meteorol. Soc. 96, 2059–2077. https://doi.org/10.1175/BAMS-D-14-00110.1.

Talukdar, S., Venkat Ratnam, M., Ravikiran, V., Chakraborty, R., 2019. Influence of black carbon aerosol on the atmospheric instability. J. Geophys. Res. https://doi.org/10.1029/2018JD029611.

Van der Zee, S.C., Fischer, P.H., Hoek, G., 2016. Air pollution in perspective: health risk s of air pollution expressed in equivalent numbers of passively smoked cigarettes. Environ. Res. 148, 475–483. https://doi.org/10.1016/j.envres.2016.04.001.

Weyant, C.L., Shepson, P.B., Subramanian, R., Cambaliza, M.O.L., Heimburger, A., McCabe, D., Baum, E., Stirm, B.H., Bond, T.C., 2016. Black carbon emissions from associated natural gas flaring. Environ. Sci. Technol. 50 (4), 2075–2081. https://doi.org/10.1021/acs.est.5b04712, 2016.

Wu, J., Lu, J., Min, X., Zhang, Z., 2018. Distribution and health risks of aerosol black carbon in a representative city of the Qinghai-Tibet Plateau. Environ. Sci. Pollut. Res. 25, 19403. https://doi.org/10.1007/s11356-018-2141-9.

Xu, J.-W., Martin, R.V., Morrow, A., Sharma, S., Huang, L., Leaitch, W.R., Burkart, J., Schulz, H., Zanatta, M., Willis, M.D., Henze, D.K., Lee, C.J., Herber, A.B., Abbatt, J.P. D., 2017. Source attribution of Arctic black carbon constrained by aircraft and surface measurements. Atmos. Chem. Phys. 17, 11971–11989. https://doi.org/10.5194/acp-17-11971-2017.

Zhang, K.M., Allen, G., Yang, B., Chen, G., Gu, J., Schwab, J., Felton, D., Rattigan, O., 2017. Joint measurements of PM2. 5 and light-absorptive PM in wood smoke-dominated ambient and plume environments. Atmos. Chem. Phys. 17, 11441–11452. https://doi.org/10.5194/acp-17-11441-2017.

Zotter, P., Herich, H., Gysel, M., El-Haddad, I., Zhang, Y., Močnik, G., Hüglin, C., Baltensperger, U., Szidat, S., Prévôt, A.S.H., 2017. Evaluation of the absorption Ångström exponents for traffic and wood burning in the Aethalometer-based source apportionment using radiocarbon measurements of ambient aerosol. Atmos. Chem. Phys. 17, 4229–4249. https://doi.org/10.5194/acp-17-4229-2017.